Long-Range Forecasting of Colorado Streamflows Based on Hydrologic, Atmospheric, and Oceanic Data

Jose D. Salas[1]; Chongjin Fu[2]; and Balaji Rajagopalan[3]

Abstract: Climatic fluctuations have profound effects on water resources variability in the western United States. The research reported herein centers on streamflow predictability at the medium- and long-range scales in rivers that originate in Colorado. Specifically, we want to improve forecasting seasonal and yearly streamflows based on atmospheric-oceanic forcing factors, such as geopotential height, wind, and sea surface temperature, as well as hydrologic factors, such as snow water equivalent. The approach followed in the study involves searching for potential predictors, applying principal component analysis (PCA) and multiple linear regression (MLR) for forecasting at individual sites, canonical correlation analysis (CCA) for forecasting at multiple sites, and testing the forecasts using various performance measures. The analysis includes comparisons of forecasts by using various combinations of possible predictors, such as hydrologic, atmospheric, and oceanic variables. The study brought into relevance the significant benefits of using atmospheric, oceanic, and hydrological predictors for long-range streamflow forecasting. It has been shown that forecasts based on PCA applied to individual sites give very good results for both seasonal and yearly timescales. We also found that although PCA has been applied on a site-by-site basis, the forecasts approximated well the historical cross correlations, although some underestimation was noted for two sites. Furthermore, the forecasts based on CCA were less efficient than those based on PCA. **DOI: 10.1061/(ASCE)HE.1943-5584.0000343.**

CE Database subject headings: Forecasting; Streamflow; Stochastic processes; Colorado; Hydrologic data.

Author keywords: Forecasting streamflows; Atmospheric/oceanic predictors; Flow prediction; Stochastic analysis; PCA; CCA.

Introduction

Although the state of Colorado is located in a semiarid climate, it has important water resources because of its high elevation and significant amount of snowfall every year. Several major rivers originate in Colorado, such as the Colorado, Arkansas, and Rio Grande. Agriculture, municipal water supply, hydropower generation, and recreational activities from the headwater regions heavily rely on streamflows. Water demand has been increasing as the western states continue to develop and the population continues to grow. Thus, balancing a limited and variable water supply and competing increasing water demands must be tackled by water resources managers to make a sufficient amount of water available when it is needed. However, water availability is highly affected by hydroclimatic events. Understanding the predictability of such phenomena is the main focus of the research reported here.

There is growing evidence of the effects of atmospheric-oceanic features on the hydrology of the western basins (e.g., Piechota et al. 1997; McCabe and Dettinger 1999; Regonda et al. 2006). Quantifying such effects in the headwaters of Colorado rivers is difficult because of the varied topography in the Rocky Mountains. The rivers that originate in the Colorado and flow downstream across semiarid and arid lands are prone to frequent periods of low flows. As important sources of water supply for many users, the rivers have been developed and controlled with many river diversions and dams. Operating such systems requires reliable streamflow forecasts. Every year, management decisions (for operating the systems) are made early in the year in anticipation of the forthcoming spring and summer streamflows. Thus, long-range streamflow forecasting is of particular interest for improving system operations.

Colorado is a mountainous region, and a major source of streamflows is melting snow. Thus, snowfall and the ensuing snowpack in the preceding months of the season of interest are important factors for streamflow forecasting. However, several other factors affect the fluctuations of streamflows, such as the water content in the atmosphere and its transportation to the area of interest. For example, geopotential height (GH) is an indicator of the conditions leading to precipitation and eventually streamflows. Also, temperature and humidity are very much related to the amount of moisture in the air, and wind is a determinant factor for moisture transport in the atmosphere. Likewise, as the oceans are the largest resource of water on earth, ocean dynamics play a significant role in streamflow variability. Perhaps the most important variable representing oceanic conditions is sea surface temperature (SST), and many oceanic climatic indexes have been developed, such as the Pacific Decadal Oscillation (PDO) index. Because streamflow is part of the global water circulation, its variability is very much related to those of atmospheric and oceanic conditions. Thus, streamflow-forecast models must include key atmospheric and oceanic variables as predictors, in addition to hydrological variables.

The scope of the study described herein centers on streamflow predictability at the seasonal and yearly scales in the headwaters of rivers that originate in Colorado. To this end, the specific objective of the study has been to develop and assess models and methods for forecasting seasonal April through July (Apr.–Jul.) and yearly

[1]Professor, Dept. Civil and Environmental Engineering, Colorado State Univ., Fort Collins, CO 80523.

[2]Graduate Student, Dept. Civil and Environmental Engineering, Colorado State Univ., Fort Collins, CO 80523 (corresponding author). E-mail: cfu@engr.colostate.edu

[3]Professor, Dept. Civil and Architectural Engineering, Univ. of Colorado, Boulder, CO 80523.

Note. This manuscript was submitted on February 26, 2010; approved on October 12, 2010; published online on October 28, 2010. Discussion period open until November 1, 2011; separate discussions must be submitted for individual papers. This paper is part of the ***Journal of Hydrologic Engineering***, Vol. 16, No. 6, June 1, 2011. ©ASCE, ISSN 1084-0699/2011/6-508–520/$25.00.

April through March (Apr.–Mar.), October through September (Oct.–Sep.), January through December (Jan.–Dec.), and February through January (Feb.–Jan.) streamflows for the Yampa, Gunnison, San Juan, Poudre, Arkansas, and Rio Grande Rivers. The models will include forecasting at single and multiple sites. The forecasts will be based on identifying hydrologic predictors, such as snow water equivalent (SWE); atmospheric predictors, such as GH and wind; and oceanic predictors, such as SST. This study builds on previous studies in which the effects of climatic variables have been identified to be useful for long-range forecasting of hydrological variables such as streamflows. The main contribution of our study is to quantify the role and effect that each group of predictors has on long-range streamflow forecasting and the effect of the beginning of the year in forecast efficiency. This may be particularly useful in cases of ungauged basins in which hydrologic predictors may not be readily available.

Brief Review of Related Studies

Existing medium- and long-range streamflow-forecast models for Colorado rivers commonly rely on multiple linear regression, where previous records of SWE, precipitation, and streamflows are used as predictors. In studies of the Rio Grande basin, Haltiner and Salas (1988) and Wang and Salas (1991) showed that significant improvements in forecasting efficiency can be achieved using time-series analysis techniques. Also, literature has demonstrated the significant effects of climatic signals, such as SST, ENSO, and PDO, on precipitation and streamflow variations (e.g., Cayan and Webb 1992; Mantua et al. 1997; Clark et al. 2001; Hidalgo and Dracup 2003), and that seasonal and longer-term streamflow forecasts can be improved using climatic factors (e.g., Hamlet and Lettenmaier 1999; Clark et al. 2001; Eldaw et al. 2003; Grantz et al. 2005; Tootle et al. 2007). Thus, the literature suggests that it may be worthwhile to examine in closer detail forecasting schemes that include not only the usual hydrologic predictors (e.g., SWE) but also climatic factors that may improve streamflow forecasting in the headwaters of Colorado streams. Also, previous studies suggested that despite the influence of major climatic factors, such as ENSO, on the hydrology of the Colorado River Basin, there are significant differences in their effects from basin to basin (McCabe and Dettinger 2002). For this reason, in our research we considered three streams in the Colorado River headwaters (Yampa, Gunnison, and San Juan), and three other rivers that flow in other directions (Poudre, Arkansas, and Rio Grande.)

Studies have pointed out the connections between the extreme phases of ENSO and the fluctuations of precipitation and streamflow in various parts of the world (e.g., Ropelewski and Halpert 1987; Cayan et al. 1998). For example, significant relationships were found between El Niño and extreme drought years in the Pacific Northwest and between La Niña events and dry conditions in the southern United States (e.g., Piechota and Dracup 1996). Also, during El Niño above-normal precipitation was found in the desert Southwest (e.g., Cayan and Webb 1992; Dettinger et al. 1998). In forecasting studies of precipitation and air temperature in the United States based on ENSO, SST, tropical precipitation (TP), GH, winds, and the Artic Oscillation (AO), Higgins et al. (2000) found that TP and AO were the dominant factors. Also, ENSO influences have been observed on snow water equivalent (Clark et al. 2001) and streamflows (e.g., Piechota et al. 1997). In studying the Mississippi River, Maurer and Lettenmaier (2003) found that in the eastern part of the basin and for 3 months or greater lead times, ENSO and AO indexes were more important than land-surface-state indicators, such as soil moisture and snow. Also, Maurer et al. (2004) studied the predictability of seasonal runoff in the continental United States between 25° and 53°N as a function of North Atlantic Oscillation (NAO), North Pacific Pattern (NP), Pacific North American (PNA) index, Atlantic Multidecadal Oscillation (AMO), AO, Niño 3.4, and PDO and found that the positive phase of El Niño 3.4 was useful for forecasting the March to May runoff, while a negative phase Niño 3.4 was useful for forecasting the December to February runoff. Furthermore, effects on decadal timescales primarily driven by the PDO have been found (e.g., Mantua et al. 1997; McCabe and Dettinger 1999; McCabe et al. 2004).

Moss et al. (1994) used the Southern Oscillation Index (SOI) as a predictor of the probability of low flows in New Zealand. Eltahir (1996) showed that up to 25% of the natural variability of the Nile River annual flows is associated with ENSO events, and Eldaw et al. (2003) reported that SST in the Pacific and Atlantic oceans and precipitation at Guinea Gulf were very useful for long-range forecasting of seasonal streamflows in the Blue Nile River. Also, Salas et al. (2005) in studying droughts in the Poudre River, utilized SSTs in the Pacific to forecast the next years flows that may occur in the basin. And, Grantz et al. (2005) developed a forecast model using SST, GH, and SWE as predictors for forecasting April to July streamflows at the Truckee and Carson rivers in Nevada. They found that forecast skills are significant for up to 5 months lead time based on SST and GH. Also, Regonda et al. (2006) reported successful streamflow forecasts in the Gunnison River by using various climatic factors. Tootle and Piechota (2006) studied the connections between the Pacific and Atlantic SSTs and streamflows in the United States. Tootle et al. (2005), in a study of 639 U.S. rivers, found significant relationships between ENSO, PDO, AMO, and NAO indexes and streamflows, which suggested that they may be useful for streamflow forecasts. In addition, Canon et al. (2007) studied the Colorado River and found significant relationships between SPI (standardized precipitation index), PDO, and BEST (bivariate ENSO time series). And, Sveinsson et al. (2008) studied the variability of spring streamflows in the Quebec region and suggested that they are influenced by SSTs, winds, and pressure in the Pacific and Atlantic oceans, as well as by winds and pressure over the Arctic and North America.

Study Area and Data

Six streamflow sites in rivers that originate in the state of Colorado were selected for the study. They include the Arkansas, Gunnison, Poudre, Rio Grande, San Juan, and Yampa rivers. Fig. 1 shows the locations of the sites, and additional information is given in Table 1. The data for Poudre are naturalized streamflows from the Northern Colorado Water Conservation District; those for the Arkansas and Rio Grande are from the Hydrology and Climate Data Network (HCDN) of the USGS (Slack and Landwehr 1992); and data for the Gunnison, San Juan, and Yampa are naturalized streamflows that are available at the U.S. Bureau of Reclamation (USBR) website (http://www.usbr.gov/lc/region/g4000/NaturalFlow/index.html).

Other data, such as SWE, were obtained from the Natural Resources Conservation Services of the USDA, and the Palmer drought severity index (PDSI) from the National Climatic Data Center (NCDC) of the National Oceanic and Atmospheric Administration (NOAA). In addition, the atmospheric and oceanic data were obtained from NOAA's Climate Diagnostic Center website (http://www.cdc.noaa.gov). They include climatic data such as SST, GH, temperature, relative humidity (RH), outgoing longwave radiation (OLWR), and wind, which are available on a $2.2° \times 2.2°$ grid worldwide from the NCEP-NCAR reanalysis

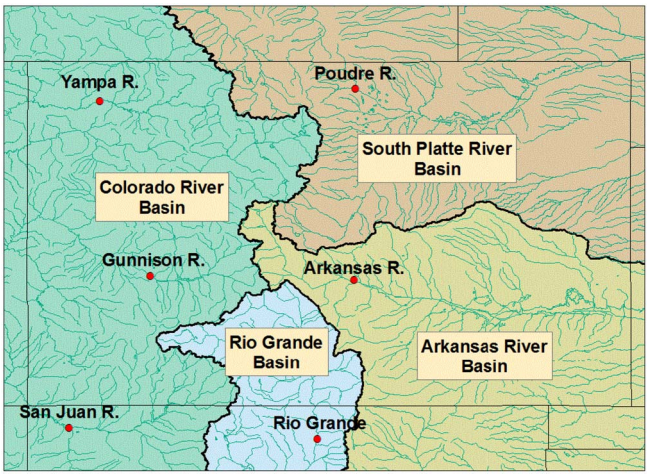

Fig. 1. Map of study area and flow sites

(Kalnay et al. 1996). Furthermore, key climatic indexes, such as SOI, PDO, NAO, and the SST observations for the El Niño regions are also available from the same source. The data length used for the study is 53 years (1949–2001).

Methodology

The approach followed in the research included searching for potential predictors, applying MLR and principal component analysis (PCA) for forecasting at single sites, and using canonical correlation analysis (CCA) for forecasting at multiple sites. The forecast models have been tested in two modes: fitting and evaluation. The approach assumes that a suitable number of hydrologic, atmospheric, and oceanic predictors can be found to forecast streamflows for different time frames and river sites in the study area. The potential hydrologic predictors include SWE, precipitation, streamflows, and PDSI. The potential atmospheric predictors include variables such as GH (700 mb); meridional wind (MW) and zonal wind (ZW) at 700 mb; air temperature (AT); OLWR; RH; and AO, SOI, and NAO indexes. The oceanic predictors include variables such as PDO, SST, and SSTs related to El Niño-1, 2, 3, 4, and 3.4.

Correlation Analysis for Selecting Potential Predictors

Correlation analysis between the predictand (streamflow data) and the potential predictors were performed. A potential predictor, e.g., SST at a given location (pixel), is defined at a time period lagged before the time period specified for the predictand. For example, if we wish to forecast the total flows for the period April through July, then possible predictors may be the average SST for the preceding months, i.e., SST(JFM), SST(OND), SST(ONDJFM), and so on (where OND is the period October through December of the previous year). Because there are many potential predictors, those selected for further analysis have statistical significant correlations. For those variables that are available worldwide for every pixel (e.g., GH), correlation maps are created that use color codes to show the values of the correlations. From these maps, areas not less than 5°× 5° with significant correlations are identified and selected as the potential predictors. Also, for other variables, such as SWE and PDO where correlation maps are not applicable, the same statistical criterion for selecting potential predictors is utilized. The significance of the correlation between the streamflow data and the predictor considered is determined from $r_c = t_{.95}/\sqrt{t_{.95}^2 + N - 2}$, where r_c = critical correlation coefficient; $t_{.95}$ = 95% quantile of the t-distribution with $N - 2$ degrees of freedom; and N = sample size. Thus, a potential predictor is selected for further analysis if the calculated correlation coefficient r (in absolute value) is larger than r_c. In all cases, the sample size of the data used in this study is 53 (1949–2001), therefore, the critical correlation coefficient is approximately 0.27.

Principal Component Analysis

Although PCA and CCA methods are well known in literature (e.g., Manly 1994; Wilks 2006), they are summarized here for the benefit of readers and ease of explanation. In PCA, a linear transformation is made on the potential predictors to obtain uncorrelated Principal Components (PCs). Consider the vector of p standardized variables $\boldsymbol{x}_1 = [\boldsymbol{x}_1 \boldsymbol{x}_2 \ldots \boldsymbol{x}_p]$. A linear transformation can be made as $z_j = \boldsymbol{x}\boldsymbol{W}$, i.e.,

$$z = \boldsymbol{x}_1 w_{1j} + \boldsymbol{x}_2 w_{2j} + \cdots + \boldsymbol{x}_p w_{pj}, \qquad j = 1, \ldots, pj \tag{1}$$

where $\boldsymbol{z}$ and $\boldsymbol{x}$ are $1 \times p$ vectors and $\boldsymbol{W}$ is a $p \times p$ coefficient matrix given by

$$\boldsymbol{W} = [\boldsymbol{w}_1 \boldsymbol{w}_2 \ldots \boldsymbol{w}_p] = \begin{bmatrix} w_{11} & w_{12} & \cdots & w_{1p} \\ w_{21} & w_{22} & \cdots & w_{2p} \\ \vdots & \vdots & \ddots & \vdots \\ w_{p1} & w_{p2} & \cdots & w_{pp} \end{bmatrix} \tag{2}$$

Thus the $\boldsymbol{x}$ variables are transformed to the $\boldsymbol{z}$ variables, which are called the PCs of $\boldsymbol{x}$.

Suppose there are N observations for each of the variables $\boldsymbol{x}_1, \ldots, \boldsymbol{x}_p$. Then, $\boldsymbol{x}$ is an $N \times p$ matrix representing the data of the p variables and $\boldsymbol{z}$ is another $N \times p$ matrix. Thus, the $\boldsymbol{z}$ variables $z_1, z_2, \ldots, z_p$ (PC *scores*) are obtained from Eq. (1). It may be shown that the columns of the $\boldsymbol{W}$ matrix are the eigenvectors corresponding to each eigenvalue of the variance-covariance matrix of the $\boldsymbol{x}$ variables, i.e., $\boldsymbol{S}_{xx} = (\boldsymbol{x}^T\boldsymbol{x})/(N-1)$ where $\boldsymbol{S}_{xx}$ is a $p \times p$ symmetric matrix. The eigenvalues of $\boldsymbol{S}_{xx}$, i.e., $\lambda_1, \ldots, \lambda_p$ can be found by solving the determinant equation $|\boldsymbol{S}_{xx} - \lambda \boldsymbol{I}| = 0$ where $\boldsymbol{I}$ is the $p \times p$

Table 1. Brief Description of River Basins and Stream Gauging Stations Utilized in Study

River and site names	Basin	USGS ID	Coordinates		Elevation (ft)	Drainage area (mi^2)
			Latitude	Longitude		
Cache la Poudre River at Mouth of Canyon, CO	South Platte	06752000	40°39′52″	105°13′26″	5,220	1,056
Arkansas River at Canon City, CO	Arkansas	07096000	38°26′02″	105°15′24″	5,342	3,117
Gunnison River above Blue Mesa Dam, CO	Colorado	09124700	38°27′08″	107°20′51″	7,149	3,453
Rio Grande below Taos Junction Bridge near Taos, NM	Rio Grande	08276500	36°19′12″	105°45′14″	6,050	9,730
San Juan River near Archuleta, NM	Colorado	09355500	36°48′05″	107°41′51″	5,653	3,260
Yampa River near Maybell, CO	Yampa-White	09251000	40°30′10″	108°01′58″	5,900	3,410

identity matrix. Then, the eigenvectors $\boldsymbol{w}_i$ corresponding to each eingenvalue λ_i are determined by solving $((\boldsymbol{S}_{xx} - \lambda_i \boldsymbol{I})\boldsymbol{w}_i = 0$, $i = 1, 2, \ldots, p$. To have nontrivial solutions, the following constraint $\boldsymbol{w}_i^T \boldsymbol{w}_i = 1$ must hold because we assumed the original data was standardized.

In summary, PCA amounts to solving for the eigenvalues of matrix $\boldsymbol{S}_{xx}$ then solving for the eigenvectors corresponding to each eigenvalue, and the PC scores are obtained from Eq. (1). After obtaining the PCs, one must decide on how many of them are to be used for further analysis. One criterion is to select the PCs that explain a given amount of the variance. Further selection may be made using stepwise regression. Detailed procedures using PCs as the predictors in a multiple linear-regression framework are given in a subsequent section.

Canonical Correlation Analysis

CCA is a method used to determine the relationship between two groups of variables. Assume p = independent variables $\boldsymbol{x} = [\boldsymbol{x}_1 \boldsymbol{x}_2 \ldots \boldsymbol{x}_p]$ and q = dependent variables $[\boldsymbol{y} = [\boldsymbol{y}_1 \boldsymbol{y}_2 \ldots \boldsymbol{y}_q]$, where $\boldsymbol{x}$ = $1 \times p$ vector; $\boldsymbol{y}$ = $1 \times q$ vector; and each $\boldsymbol{x}_i$ and $\boldsymbol{y}_i$ = column vectors of observations, i.e., vectors of size $1 \times N$. CCA creates two new variables $\boldsymbol{u} = [\boldsymbol{u}_1 \boldsymbol{u}_2 \ldots \boldsymbol{u}_n]$ and $\boldsymbol{v} = [\boldsymbol{v}_1 \boldsymbol{v}_2 \ldots \boldsymbol{v}_n]$, where $n = \min(p, q)$, i.e., $\boldsymbol{u}$ and $\boldsymbol{v}$ = $1 \times n$ vectors, and each $\boldsymbol{u}_i$ and $\boldsymbol{v}_j$ = column vectors of size $1 \times N$. The $\boldsymbol{u}$ variables are formed by a linear combination of the $\boldsymbol{x}$ variables, i.e., $\boldsymbol{u} = \boldsymbol{x}\boldsymbol{a}$, where $\boldsymbol{a} = p \times n$ matrix and the $\boldsymbol{v}$ variables are formed by a linear combination of the $\boldsymbol{y}$ variables, i.e., $\boldsymbol{v} = \boldsymbol{y}\boldsymbol{b}$ where $\boldsymbol{b} = q \times n$ matrix. It follows that

$$\boldsymbol{u}_j = \boldsymbol{x}_1 a_{1j} + \boldsymbol{x}_2 a_{2j} + \cdots + \boldsymbol{x}_p a_{pj}, \qquad j = 1, \ldots, n \tag{3}$$

and

$$\boldsymbol{v}_j = \boldsymbol{y}_1 b_{1j} + \boldsymbol{y}_2 b_{2j} + \cdots + \boldsymbol{y}_q b_{qj}, \qquad j = 1, \ldots, n \tag{4}$$

where the transformation matrices $\boldsymbol{a}$ and $\boldsymbol{b}$ are given by

$$\boldsymbol{a} = \begin{bmatrix} a_{11} & a_{12} & \ldots & a_{1n} \\ a_{21} & a_{22} & \ldots & a_{2n} \\ \vdots & \vdots & \vdots & \vdots \\ a_{p1} & a_{p2} & \ldots & a_{pn} \end{bmatrix} \qquad \boldsymbol{b} = \begin{bmatrix} b_{11} & b_{12} & \ldots & b_{1n} \\ b_{21} & b_{22} & \ldots & b_{2n} \\ \vdots & \vdots & \vdots & \vdots \\ b_{q1} & b_{q2} & \ldots & b_{qn} \end{bmatrix}$$

The variables $\boldsymbol{u}$ and $\boldsymbol{v}$ are called canonical variates and are paired so that $\boldsymbol{u}_1$ and $\boldsymbol{v}_1$ are correlated with the so-called *canonical correlation coefficient* ρ_1, then, $\boldsymbol{u}_2$ and $\boldsymbol{v}_2$ are correlated with ρ_2, etc. A schematic description of CCA is

$$\left.\begin{matrix} \boldsymbol{y}_1 \\ \boldsymbol{y}_2 \\ \vdots \\ \boldsymbol{y}_q \end{matrix}\right\} = \boldsymbol{y}^T \rightarrow \boldsymbol{y}\boldsymbol{b} = \boldsymbol{v} \rightarrow \boldsymbol{v}^T = \left\{\begin{matrix} \boldsymbol{v}_1 & \leftarrow \rho_1 \rightarrow & \boldsymbol{u}_1 \\ \boldsymbol{v}_2 & \leftarrow \rho_2 \rightarrow & \boldsymbol{u}_2 \\ \vdots & \ldots & \vdots \\ \boldsymbol{v}_n & \leftarrow \rho_n \rightarrow & \boldsymbol{u}_n \end{matrix}\right\} = \boldsymbol{u}^T \leftarrow \boldsymbol{u} = \boldsymbol{x}\boldsymbol{a} \leftarrow \boldsymbol{x}^T = \left\{\begin{matrix} \boldsymbol{x}_1 \\ \boldsymbol{x}_2 \\ \vdots \\ \boldsymbol{x}_p \end{matrix}\right.$$

where $\rho_1 > \rho_2 > \cdots > \rho_n$ (i.e., the canonical correlations have been arranged to comply with ρ_1 being the largest, and so on.) The values of the canonical variates are often called the *scores* of the canonical variates, and the matrices $\boldsymbol{a}$ and $\boldsymbol{b}$ are called *canonical loadings*.

The canonical correlation coefficients ρ and matrices $\boldsymbol{a}$ and $\boldsymbol{b}$ may be estimated as follows (Manly 1994). First, matrix $\boldsymbol{S}_a$ is obtained as $\boldsymbol{S}_a = \boldsymbol{S}_{xx}^{-1} \boldsymbol{S}_{xy} \boldsymbol{S}_{yy}^{-1} \boldsymbol{S}^T{}_{xy}$, in which $\boldsymbol{S}_{wz}$ is the covariance matrix of w and z. Then, matrix $\boldsymbol{a}$ is estimated using the eigenvalues and eigenvectors of matrix $\boldsymbol{S}_a$. Likewise, matrix $\boldsymbol{S}_b$ is determined by $\boldsymbol{S}_b = \boldsymbol{S}_{yy}^{-1} \boldsymbol{S}_{xy}^T \boldsymbol{S}_{xx}^{-1} \boldsymbol{S}_{xy}$, and matrix $\boldsymbol{b}$ is obtained by calculating the eigenvalues and eigenvectors of matrix $\boldsymbol{S}_b$. It may be shown that the eigenvalues of matrix $\boldsymbol{S}_b$, i.e., $\lambda_1, \ldots, \lambda_n$ are related to the canonical correlation coefficients $\rho' s$ as $\lambda_1 = \rho_1^2, \lambda_2 = \rho_2^2, \ldots, \lambda_n = \rho_n^2$.

The significance of the canonical correlation coefficients may be tested considering the null hypothesis $\boldsymbol{H_0} : \rho_1 = \rho_2 = \cdots = \rho_r = 0$ against the alternative hypothesis $\boldsymbol{H}_a$: at least $\rho_i \neq 0$, $i = 1, 2, \ldots, r$, where r is taken successively as $r = 1, \ldots, n$. The test statistic is (Manly 1994)

$$C = -\left[n - \frac{1}{2}(p + q + 6)\right] \times \sum_{i=1}^{r} \ln(1 - \rho_i^2) \tag{5}$$

which is χ^2 distributed with $p \times q$ degrees of freedom. A large value of C suggests that the null hypotheses must be rejected. After testing for the significance of the $\rho' s$, the relationships between the $\boldsymbol{v}$ and the $\boldsymbol{u}$ are established by fitting simple linear regressions as

$$\boldsymbol{v}_i = \beta_i \boldsymbol{u}_i, \qquad i = 1, \ldots, n' \tag{6}$$

where the $\beta_i, i = 1, \ldots, n'$ = parameters of the regression equations, and $n' \leq n$ = number of significant canonical correlations. Then, the forecast for $\boldsymbol{y}$ is obtained by inverting $\boldsymbol{v} = \boldsymbol{y}\boldsymbol{b}$ as

$$\boldsymbol{y} = \boldsymbol{v}\boldsymbol{b}^{-1} \tag{7}$$

Detailed procedures for the models using CCA are given in subsequent sections of this paper.

Forecast Models for Single Sites

Stepwise-regression analysis was applied for specifying the forecast model at single sites. The model is fitted using either the original variables or the PCs as the predictors. The stepwise regression selects the most suitable combination of predictors and the forecast model based on MLR is written as

$$\hat{y} = \sum_{j=1}^{m} \beta_j x_j \tag{8}$$

where $\hat{y}$ = streamflow forecast (standardized), β_i, $i = 1, \ldots, m$ = parameters; x_i, $i = 1, \ldots, m$ = predictors, such as SST and SWE (standardized); and m = number of predictors.

Alternatively, the forecast model using MLR can be set up based on PCs as the predictors as

$$\hat{y} = \sum_{i=1}^{m} \beta_i PC_i \tag{9}$$

where $\hat{y}$ = streamflow forecast (standardized), $\beta_i, i = 1, \ldots, m$ are the parameters, and $PC_i, i = 1, \ldots, m$ are the predictors (principal components). The PCs in Eq. (9) are obtained using stepwise regression analysis.

Forecast Models for Multiple Sites

One may perform CCA analysis by following the procedure previously outlined for all the potential predictors that may be applicable for all six sites. However, because the number of potential predictors was large, before CCA, a preorthogonal analysis was made, where PCA was performed on the potential predictors to reduce the dimensionality of the problem. Thus, CCA was conducted based on PCs (instead of the original variables) and the performance of the CCA model relied on which PCs were used. Although the first several PCs may account for the majority of the variances, not all of them may be good predictors for the CCA model. To select the PCs, the model residuals were analyzed. The sum of squared residuals *SSR* is computed as

$$SSR = \sum_{j=1}^{q} \sum_{i=1}^{N} (\hat{y}_i^j - y_i^j)^2 \tag{10}$$

where $\hat{y}_i^j$ = forecasted flows; y_i^j = observed flows; i = time; j = site; and N and q = total number of time steps and sites, respectively. The PCs that cause an increase of SSR are eliminated from the forecast model. After the PCs of the predictors are selected, CCA is then carried out based on the streamflows and the selected PCs. Significance tests are then conducted for the canonical correlation coefficients between the canonical variate pairs as indicated in the "Canonical Correlation Analysis" section.

Next, the relationships between the pairs of canonical variates $\boldsymbol{v}$ and $\boldsymbol{u}$ are established, as in Eq. (6), where $\boldsymbol{v}$ and $\boldsymbol{u}$ = canonical variates used in the CCA model [obtained from Eqs. (3) and (4), respectively]. To perform the forecasts, Eq. (3) is applied to obtain $u_1, \ldots, u_{n'}$ given the predictors $x_1, \ldots, x_p$ (now in the form of PCs), and the values v_i are obtained from Eq. (6). They are inverted back to the real space by Eq. (7) as $\hat{\boldsymbol{y}} = \boldsymbol{vb}^{-1}$. If PCs for the streamflows were used for the CCA model, then another inversion would be needed to retrieve the streamflows from the forecasted PCs.

Model Performance: Fitting and Validation Analysis

The coefficient of determination R^2 and its adjusted value R_a^2 are used for measuring the performances of forecast models. They are calculated as (Donald and Lindgren 1996)

$$R^2 = 1 - \frac{\sum_{i=1}^{N} (\hat{y}_i - y_i)^2}{\sum_{i=1}^{N} (y_i - \bar{y})^2} \tag{11}$$

$$R_a^2 = 1 - [(1 - R^2)(N - 1)/(N - m - 1)] \tag{12}$$

where $\hat{y}_i$ = forecasted streamflow; y_i = observed streamflow; $\bar{y}$ = mean of the observations; N = number of observations; and m = number of parameters. We also used the forecast skill scores Accuracy (AC) and Heidke Skill Scores (HSS). AC indicates the fraction of the forecasts that are in the same category as the observations (the streamflow categories are determined based on the 25th, 50th, and 75th percentiles.) It is given by (Wilks 2006)

$$AC = \frac{1}{N} \sum_{i=1}^{k} n(F_i O_i) \tag{13}$$

where $n(F_i O_i)$ = number of the forecasts that are in the same category i as the corresponding observations, and k = number of categories. AC ranges between 0 and 1, where 1 indicates a perfect forecast. HSS measures the fraction of correct forecasts after eliminating those that would be correct because of purely random chance. It is given by (Wilks 2006) as

$$HSS = \frac{\frac{1}{N}\sum_{i=1}^{k} n(F_i O_i) - \frac{1}{N^2}\sum_{i=1}^{k} n(F_i) n(O_i)}{1 - \frac{1}{N^2}\sum_{i=1}^{k} n(F_i) n(O_i)} \tag{14}$$

where $n(F_i)$ and $n(O_i)$ = number of forecasts and observations in category i. HSS ranges from $-\infty$ to 1. A value of 0 indicates no forecast skill and 1 indicates a perfect forecast.

In evaluating the performance of the forecast models, two procedures were utilized. In the first one (fitting method), a forecast model is fitted based on the total data, which is then applied to forecast the streamflows successively. In the second one procedure, part of the streamflow data are removed from the historical sample and a model is fitted based on the remaining data, which is then applied for forecasting the streamflows that were removed. Thus, the forecast errors can be evaluated. Subsequently, the removed data are put back into the original data set and a second part of the data are removed, a model is fitted based on the remaining data, and the 2nd model is now used to forecast the 2nd set of values removed and to estimate the ensuing forecast errors. And this procedure continues until the data set permits. For example, in the drop-1 approach, a single data is removed at a time, and the model fitting and forecast error evaluation are determined one at a time. Another example is the drop-10% approach where 10% of the data set are dropped each time and the model fitting, forecast, and error estimation are made successively, as previously explained.

Results and Discussion

The basic statistics of the April to July streamflows for the 6 study sites were calculated (not shown because of space limitation). The means of the streamflows for these sites fell basically into two groups, the first one (Poudre and Arkansas) approximately 200,000 to 400,000 m^3 [thousand acre-feet (TAF)] and the second (Gunnison, San Juan, Rio Grande, and Yampa) approximately 700 to 1,000 m^3 TAF. The coefficients of variation for all sites were less than 1, and the lag-1 correlation coefficients were generally small (less than 0.25). The skewness coefficients varied from 0.27 to 1.30, and logarithmic transformations were needed to decrease the skewness for some sites. Table 2 gives the cross-correlation coefficients of the April to July streamflows for the six sites, which vary in from 0.41 to 0.95. As expected, the magnitude of the correlations becomes smaller as the distance between the stations increases. Also, similar basic statistics for the annual streamflows were determined (not shown).

Table 2. Cross-Correlation Coefficients for April through July Historical Streamflows in the Study Area

Sites	Poudre	Arkansas	Gunnison	Rio Grande	San Juan	Yampa
Poudre	1	0.68	0.65	0.41	0.47	0.72
Arkansas	0.68	1	0.95	0.73	0.70	0.82
Gunnison	0.65	0.95	1	0.69	0.72	0.87
Rio Grande	0.41	0.73	0.69	1	0.88	0.46
San Juan	0.47	0.70	0.72	0.88	1	0.49
Yampa	0.72	0.82	0.87	0.46	0.49	1

Selection of Potential Predictors

Correlation analysis between the April to July streamflows and the potential predictors showed that for the 6 study sites the hydrological variables, such as SWE, generally have the highest correlations compared with those for other types of variables. The correlation coefficients between streamflows and SWE varied from 0.46 to 0.85, depending on the basin. Also, the correlations between streamflows and PDSI varied from 0.28 to 0.70. On the other hand, the correlations with the April to July streamflows of the previous year (i.e., lag-1 correlation) are small and not significant. For illustration purposes, Table 3 shows the 15 potential predictors having the highest correlations for the Gunnison River. Similar correlations were estimated for all six streamflow sites (all results are not shown). They showed that atmospheric variables, such as GH and wind, also have significant correlations with streamflows, varying from −0.67 to +0.61. For example, Fig. 2 shows the correlation map for the April to July streamflows of the Gunnison River versus the previous year October to December global GH (700 mb). It may be observed that correlations in the range from −0.50 to +0.50 and for several areas the correlations are approximately −0.45 or +0.45. The western United States has a correlation of approximately −0.45. Fig. 3 show the correlation map for the April to July streamflows versus global meridional wind (700 mb) for October to December of the previous year. It shows correlations of approximately −0.5 at the northeast Pacific and over the northwest Atlantic, while the correlations are approximately +0.5 over the eastern United States and Canada.

Furthermore, SST and some oceanic indexes, such as PDO, are significantly correlated with the April through July streamflows for some of the sites in the study area. For example, the correlation map of the April to July streamflows of the Gunnison River versus the October through December (previous year) global SST (not shown) indicated two large regions in the northern Pacific Ocean with significant correlation coefficients. One region showed positive correlation of approximately 0.45 and the other showed negative correlation of approximately −0.45. Thus, from the correlation analysis several variables having significant correlations with the streamflows were identified for each site. They were used as the potential predictors for further analysis. The number of the potential predictors for the April through July streamflow forecasts for the six sites ranged from 21 (Arkansas) to 48 (Rio Grande).

Likewise, correlation analysis was conducted for the Gunnison River yearly streamflows (October through September, January through December, February through January, and April through March) versus hydrologic, atmospheric, and oceanic variables. For example, correlation maps and tables (not shown) gave correlation coefficients in the range from −0.49 to +0.82 for April through March and −0.45 to +0.52 for Oct.–Sep. SWE is the variable with the highest correlation (0.82) for April through March yearly streamflows, but for October through September, the correlation with SWE drops to 0.33. Clearly, the time period where the year is defined is important, e.g., for the year April through March, the April 1 SWE plays a significant role because much of the runoff in the following months arises from the snowmelt that has been on the ground by April 1. On the other hand, for the year October through September, either the effect of SWE is small or not significant at all because much of the snow that has been on the ground by April 1 has been melted and does not contribute to the streamflow in the year that begins in October.

Several studies have identified the link between large-scale climatic features and regional hydroclimatic variability in North America (e.g., McCabe and Dettinger 2002; Grantz et al. 2005; Regonda et al. 2006; Tootle and Piechota 2006; Sveinsson et al. 2008). These studies have all identified large-scale climate indicators (similar to those found in this paper) and their potential for long-range streamflow forecasting. Also, these previous studies have documented not only the statistical associations between climatic factors and hydrologic variables, such as streamflows, but also provided the underlying physical mechanisms (arguments) supporting such statistical associations. For example, in studying the predictability of the Gunnison River (using similar data as we have in this study) Regonda et al. (2006) showed correlation maps between the first PC of Spring flows and Nov.–Mar. GH

Table 3. Fifteen Potential Predictors for the April through July Streamflows of the Gunnison River

No.	Name	Variable	Time	Location	General description	Corr. coef.
3	SST2	Sea surface temperature	Jan.–Mar.	25°N–30°N 155°E–175°E	Northwest Pacific, southeast of Japan	−0.45
5	SST4	Sea surface temperature	Previous Oct.–Dec.	25°N–32°N 158°E–168°E	Northwest Pacific, southeast of Japan	−0.45
11	SSST1	Seesaw SST	Jan.–Mar.		SST1-SST2	0.50
12	SSST2	Seesaw SST	Previous Oct.–Dec.		SST3-SST4	0.53
15	GH3	Geopotential height (700 mb)	Previous Oct.–Dec.	40°N–60°N 60°W–75°W	Over eastern Canada and eastern United States	0.43
19	MW1	Meridiona-1 wind (700 mb)	Previous Oct.–Dec.	35°N–55°N 80°W–95°W	Eastern Canada and eastern United States	0.51
21	MW3	Meridiona-l wind (700 mb)	Previous Oct.–Dec.	30°N–55°N 40°W–65°W	Northwest Atlantic, east of Canada and United States	−0.44
24	ZW3	Zonal wind (700 mb)	Previous Oct.–Dec.	25°N–35°N 100°W–120°W	Southern United States	0.44
26	AT1	Air temperature	Previous Oct.–Dec.	45°N–55°N 105°W–110°W	Western mountain states	−0.44
28	OLR2	Outgoing long-wave radiation	Previous Oct.–Dec.	31°N–46°N 105°W–120°W	Central states and western mountain states	−0.44
31	RH3	Relative humidity	Previous Oct.–Dec.	30°N–35°N 70°W–80°W	Southeast United States	0.48
35	PDSI1	Palmer index	Jan.–Mar.		Climate division	0.70
37	SWE1	Snowwater equivalent	Feb. 1		Basin average	0.73
38	SWE2	Snowwater equivalent	Mar. 1		Basin average	0.76
39	SWE3	Snowwater equivalent	Apr. 1		Basin average	0.85

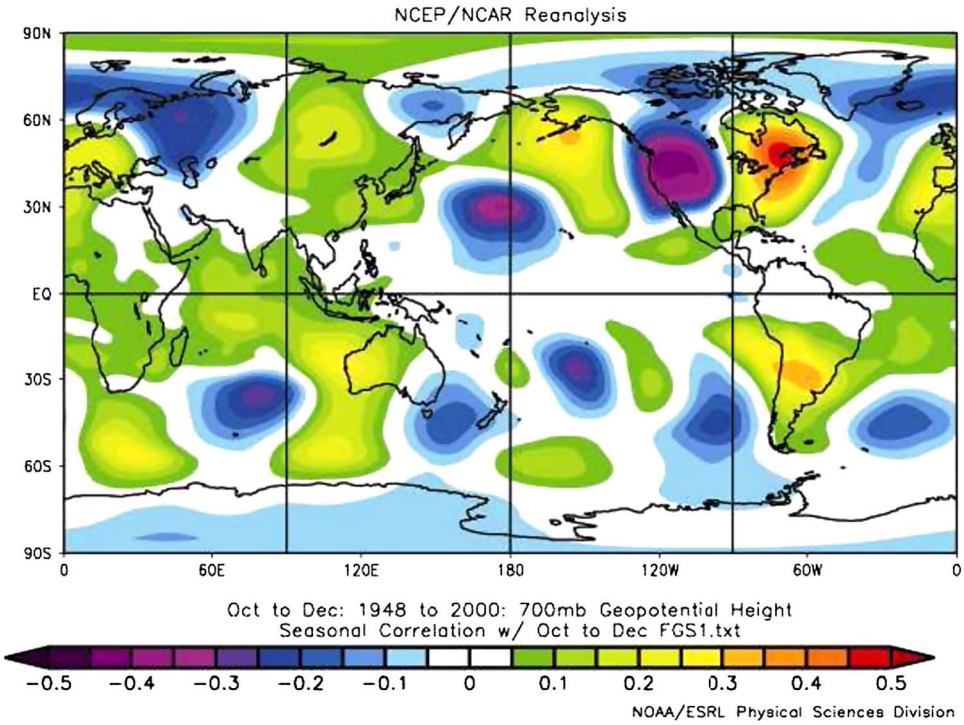

Fig. 2. Correlation map for the Apr.–Jul. streamflows of the Gunnison River and the previous year's Oct.–Dec. global 700 mb geopotential heights

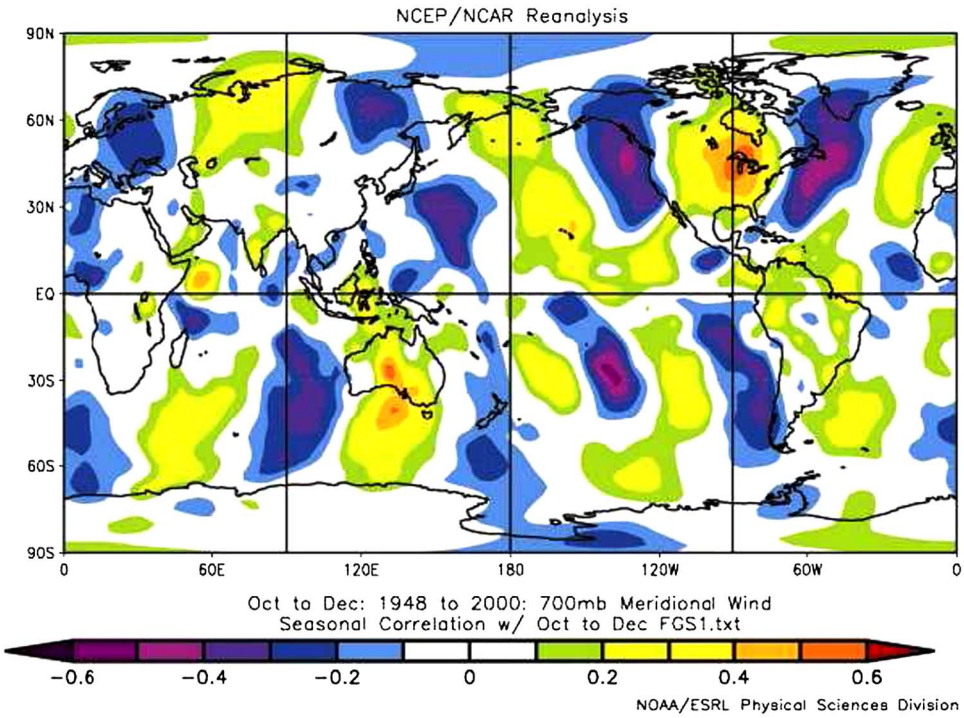

Fig. 3. Correlation map for the Apr.–Jul. streamflows of the Gunnison River and the previous year's Oct.–Dec. global meridional wind (700 mb)

(700 mb), surface air temperature, zonal and meridional winds (700 mb), and SST. Their correlation maps for GH and meridional wind [Figs. 5(a)–5(d)] are quite similar to our maps in Figs. 2 and 3, respectively. Regonda et al. also showed composite maps of vector wind (700 mb) anomalies for wet and dry years, and found that negative GH anomalies tend to direct the storm tracks into the basin, resulting in increased streamflows. They also found that correlation maps of zonal and meridional winds (700 mb) are consistent with the 700 mb GH, in that winds over the southwestern United States bring moisture into the Gunnison River Basin, leading to above-average spring streamflows. Also, Grantz et al. (2005) showed the connection between climate and streamflow by using composite analysis of sea level pressures and winds during high and low streamflow years in the western United States. The physical mechanisms as previously described are the reasons for the suite of SST-, pressure-, and wind-based predictors that emerged in

studies aimed at improving long-range streamflow forecasting based on climatic indicators. The physical arguments they provided are certainly valid for the analysis carried out in this paper.

Forecast Results for April to July Streamflows at Single Sites

MLR forecast models were built for the standardized April through July streamfllows using all variables (predictand and predictors) in their original form. For ease of reference, we refer to these forecast models (Table 4) as MLR. Generally, there are 3 to 8 predictors and as expected, SWE is the most important predictor for every site except for the Yampa River, where it is second-best. Also, atmospheric variables, such as Zonal or Meridional wind (at 700 mb), GH (700 mb), and RH, are also good predictors for most of the 6 sites. And, SST are important predictors for 4 sites (Poudre, Arkansas, Gunnison, and Rio Grande), but they are not included as predictors for the San Juan and Yampa Rivers, although for these two sites, OLRD is included. Although SST are important predictors for most sites, other oceanic indexes, such as PDO and El Niño-related indexes, were not included as predictors, which confirms the results found by Regonda et al. (2006) in their studies of the Gunnison River.

The *R*-squares and forecast skill scores for forecasting the April through July streamflows based on MLR were determined (not shown). In general, the results obtained were quite good. For example, the adjusted R^2 for the drop-1 results gave values in the 0.48–0.80, where the smaller values 0.48 and 0.49 corresponded to the Arkansas and Poudre Rivers, respectively, while values in the 0.68–0.80 range were obtained for the other four sites. Also, the forecast skill scores were quite reasonable with drop-1 AC in the 0.49–0.68 range and HSS in the 0.32–0.57 range. Considering the various metrics, it was clear that the better values were obtained for the Gunnison, Rio Grande, San Juan, and Yampa Rivers than for the Arkansas and Poudre Rivers. The cross-correlation coefficients obtained for the drop-1 forecasted April through July streamflows were somewhat lower than the historical correlations (Table 2). This was especially noticeable for the Poudre and Arkansas Rivers, where the underestimation could be as high as 32%. The lower values obtained for the cross correlations were expected because the forecasts were made on a site by site basis.

In addition, we also applied PCA on all the potential predictors for each site. Then, the PCs that explained most of the variance were used to fit a forecast model based on MLR (referred to as PCA model). The results for all sites showed that the first 15 PCs generally accounted for at least 90% of the variance. For illustration, Table 5 shows the variances of the first 15 PCs for the Gunnison River. Thus, we considered the first 15 PCs for further analysis, the other PCs were ignored, and the stepwise MLR model was applied for predicting the April through July streamflows based on PCs. Table 6 shows the PCs that were obtained for each site and the estimated model parameters. For most of the sites, the first 3 PCs are included, and the total number of PCs in the models is either 5 or 6. The performance measures of the forecasts based on PCA models are shown in Table 7. In general the forecasts using the PCA models are pretty good for most sites. The values of the drop-1 adjusted R^2 are in the 0.49–0.77 range. Again, the smallest values are 0.49 and 0.54 for the Poudre and Arkansas Rivers, respectively, and the values for the other sites varied in the 0.70–0.77 range. Also, the drop-1 forecast skill scores AC are in the 0.49–0.68 range and HSS vary from approximately 0.32–0.57. The AC values for the Poudre and Arkansas Rivers are 0.49 and 0.53, respectively, while the average AC for the other four rivers are approximately 0.61. Likewise, the HSS scores for the Poudre and Arkansas Rivers are 0.32 and 0.37, respectively, while the average HSS for the other sites are approximately 0.49. The cross-correlation coefficients of the forecasted streamflows among the six sites are shown in Table 8. As expected, the cross-correlation coefficients are somewhat smaller than those of the observed streamflows. Overall, however, the cross correlations obtained using PCA models are better than those obtained from the MLR models previously described. Furthermore, the plots comparing the historical versus the forecasted flows (not shown) suggested that the forecasts obtained based on PCA give quite good results. The various results as previously described confirm that there is some noted difference in the forecast performances of the six rivers, where the better performances are obtained for the Gunnison, Rio Grande, San Juan, and Yampa Rivers than for the Poudre and Arkansas Rivers.

Table 5. Variances of PCs of Potential Predictors for Forecasting April through July Streamflows of Gunnison River

PCs	Variance	%	Accumulation %	PCs	Variance	%	Accumulation %
1	11.50	29.5	29.5	10	1.17	3.0	80.1
2	3.77	9.7	39.2	11	0.99	2.5	82.7
3	3.09	7.9	47.1	12	0.89	2.3	85.0
4	2.77	7.1	54.2	13	0.74	1.9	86.9
5	2.40	6.2	60.3	14	0.67	1.7	88.6
6	2.12	5.4	65.8	15	0.63	1.6	90.2
7	1.69	4.3	70.1	↓	↓	↓	↓
8	1.44	3.7	73.8				
9	1.30	3.3	77.1	39	0.00	0.0	100.0

Comparing Forecasts for Various Types of Predictors

In the previous section, we assessed the forecast performances based on MLR and PCA using all the hydrologic, atmospheric,

Table 4. Models Obtained Based on MLR for Forecasting April through July Streamflows for Six Study Sites

Site	Equations
Poudre River	$y = -0.24 \times \text{SST8(A} - \text{J)} + 0.412 \times \text{ZW3(J} - \text{M)} + 0.616 \times \text{SWE3}$ (Apr. 1)
Arkansas River	$y = -0.294 \times \text{SST4(J} - \text{S)} - 0.140 \times \text{MW2(O} - \text{D)} + 0.423 \times \text{RH(O} - \text{D)} + 0.392 \times \text{SWE3}$ (Apr. 1)
Gunnison River	$y = 0.192 \times \text{SST2(J} - \text{M)} + 0.124 \times \text{SST7(A} - \text{J)} - 0.194 \times \text{SST9(A} - \text{J)} - 0.231 \times \text{GH5(O} - \text{D)} + 0.209 \times \text{ZW2(J} - \text{M)} + 0.203 \times \text{RH4(O} - \text{D)} + 0.288 \times \text{PDSI1(J} - \text{M)} + 0.518 \times \text{SWE3}$ (Apr. 1)
Rio Grande River	$y = 0.249 \times \text{SSST1(J} - \text{M)} - 0.213 \times \text{GH6(O} - \text{D)} - 0.176 \times \text{ZW4(O} - \text{D)} + 0.360 \times \text{RH2(O} - \text{D)} + 0.425 \times \text{SWE3}$ (Apr. 1)
San Juan River	$y = 0.187 \times \text{GH3(O} - \text{D)} - 0.172 \times \text{GH5(J} - \text{S)} - 0.170 \times \text{OLR1(J} - \text{M)} - 0.130 \times \text{OLR2(O} - \text{D)} + 0.623 \times \text{SWE3}$ (Apr. 1)
Yampa River	$y = -0.307 \times \text{GH1(J} - \text{M)} - 0.174 \times \text{MW3(O} - \text{D)} - 0.235 \times \textit{OLR}\text{2(J} - \text{M)} + 0.829 \times \text{PDSI1(J} - \text{M)} - 0.583 \times \text{PDSI2(O} - \text{D)} + 0.273 \times \text{SWE2}$ (Mar. 1)

Note: The parenthesis in the equations indicate the time period. For example, SST8 (A-J) indicates the SST for the time period April through June of the previous year.

Table 6. Parameters of PCA Model for Forecasting April through July Streamflows for Each Site

Poudre		Arkansas		Gunnison		Rio Grande		San Juan		Yampa	
PCs	β	PCs	β	PCs	β	PCs	β	PCs	β	PCs	β
PC1	−0.645	PC1	−0.731	PC1	−0.788	PC1	−0.809	PC1	−0.837	PC1	0.815
PC2	−0.315	PC3	0.189	PC2	−0.230	PC2	0.263	PC2	0.136	PC2	0.160
PC4	−0.173	PC4	−0.371	PC3	0.174	PC3	0.254	PC3	−0.143	PC3	0.190
PC10	0.228	PC10	−0.169	PC4	0.245	PC6	−0.160	PC7	−0.115	PC12	−0.163
PC12	−0.197	PC12	0.177	PC6	0.146	PC9	−0.152	PC8	−0.223	PC17	0.256
				PC12	0.162	PC11	0.115				

Table 7. Model Performance Measures for Forecasting April through July Streamflows Based on PCA

Method	Item	Poudre	Arkansas	Gunnison	Rio Grande	San Juan	Yampa
Fitting	R^2	0.67	0.70	0.87	0.86	0.85	0.88
	Adj. R^2	0.63	0.66	0.85	0.84	0.83	0.87
Drop-1	R^2	0.54	0.58	0.76	0.73	0.77	0.79
	Adj. R^2	0.49	0.54	0.73	0.70	0.74	0.77
Fitting	Accuracy	0.55	0.57	0.60	0.66	0.74	0.70
	HSS	0.39	0.42	0.47	0.56	0.65	0.60
Drop-1	Accuracy	0.49	0.53	0.57	0.58	0.68	0.62
	HSS	0.32	0.37	0.42	0.46	0.57	0.50

Table 8. Cross-Correlation Coefficients between April through July Drop-1 Forecasted Streamflows Based on PCA Models

Sites	Poudre	Arkansas	Gunnison	Rio Grande	San Juan	Yampa
Poudre	1	0.67	0.66	0.45	0.48	0.72
Arkansas	0.67	1	0.78	0.61	0.64	0.72
Gunnison	0.66	0.78	1	0.60	0.67	0.86
Rio Grande	0.45	0.61	0.60	1	0.82	0.56
San Juan	0.48	0.64	0.67	0.82	1	0.61
Yampa	0.72	0.72	0.86	0.56	0.61	1

and oceanic predictors. Here, we analyze the performances obtained by different groups of predictors considering the Gunnison River. For example, because SWE and PDSI are the most important predictors of streamflows from April through July, we examined the results we would obtain if we eliminated SWE and PDSI from the pool of predictors. This case is relevant especially for ungauged basins where no rainfall and snowfall data nor snowpack over the basin may be available. Thus, five cases were considered: (1) oceanic variables only, (2) atmospheric variables only, (3) oceanic and atmospheric variables only, (4) hydrologic variables only, and (5) all variables for forecasting the April through July streamflows. Table 9 gives the results of the model performances. For instance, considering the drop-1 adjusted R^2, it is clear that using oceanic predictors only gives the smallest value (0.28), while using atmospheric predictors alone gives a larger value (0.48). Using both oceanic and atmospheric predictors increases the R^2 to 0.52. In turn, using the hydrologic predictors only gives even a larger value (0.65), and using all predictors gives the highest value 0.73.

As expected, the model using all predictors has better performance than those using only the predictors of individual groups or a combination of predictors. The results are similar for the other forecast skill scores, such as AC and HSS (Table 9). But the comparison, rather than highlighting the fact that the model that includes all predictors has better performance than the others, actually points out how beneficial it may be for long-range forecasting the use of atmospheric/oceanic predictors. In addition, Fig. 4 shows the scatter plots of drop-1 forecasts based on PCA models versus historical values using each of the 5 groups of predictors (1 through 5). Comparing the plots helps us to understand the role and benefit of each group of predictors. For instance, comparing Figs. 4(a) and 4(b) it is clear the benefit of using atmospheric predictors especially in the low flow and high flow ranges. Also Fig. 4(c) suggests some improved forecasts using both oceanic and atmospheric predictors. Likewise, comparing Figs. 4 (d) and 4(e) confirm the advantage of using all predictors if they are available. Also, the importance of climatic predictors for long-range streamflow forecasting are explained in the analysis of yearly forecasts shown in a subsequent section.

Forecast Results for April through July Streamflows Based on Multisite Models

Forecast models were also fitted for all six sites simultaneously using CCA, and the results were compared with those obtained using the single-site MLR and PCA. The potential predictors that

Table 9. Model Performances Using Various Combinations of Predictors for Forecasting April through July Streamflows of the Gunnison River

		Models based on				
Method	Item	Oceanic variables	Atmospheric variables	Oceanic and atmospheric variables	Hydrological variables	All variables
Fitting	R^2	0.45	0.62	0.67	0.72	0.87
	Adj. R^2	0.41	0.59	0.65	0.71	0.85
Drop-1	R^2	0.32	0.51	0.56	0.66	0.76
	Adj. R^2	0.28	0.48	0.52	0.65	0.73
Fitting	Accuracy AC	0.43	0.47	0.50	0.54	0.60
	HSS	0.25	0.31	0.35	0.42	0.47
Drop-1	Accuracy AC	0.41	0.45	0.48	0.50	0.57
	HSS	0.23	0.29	0.32	0.37	0.42

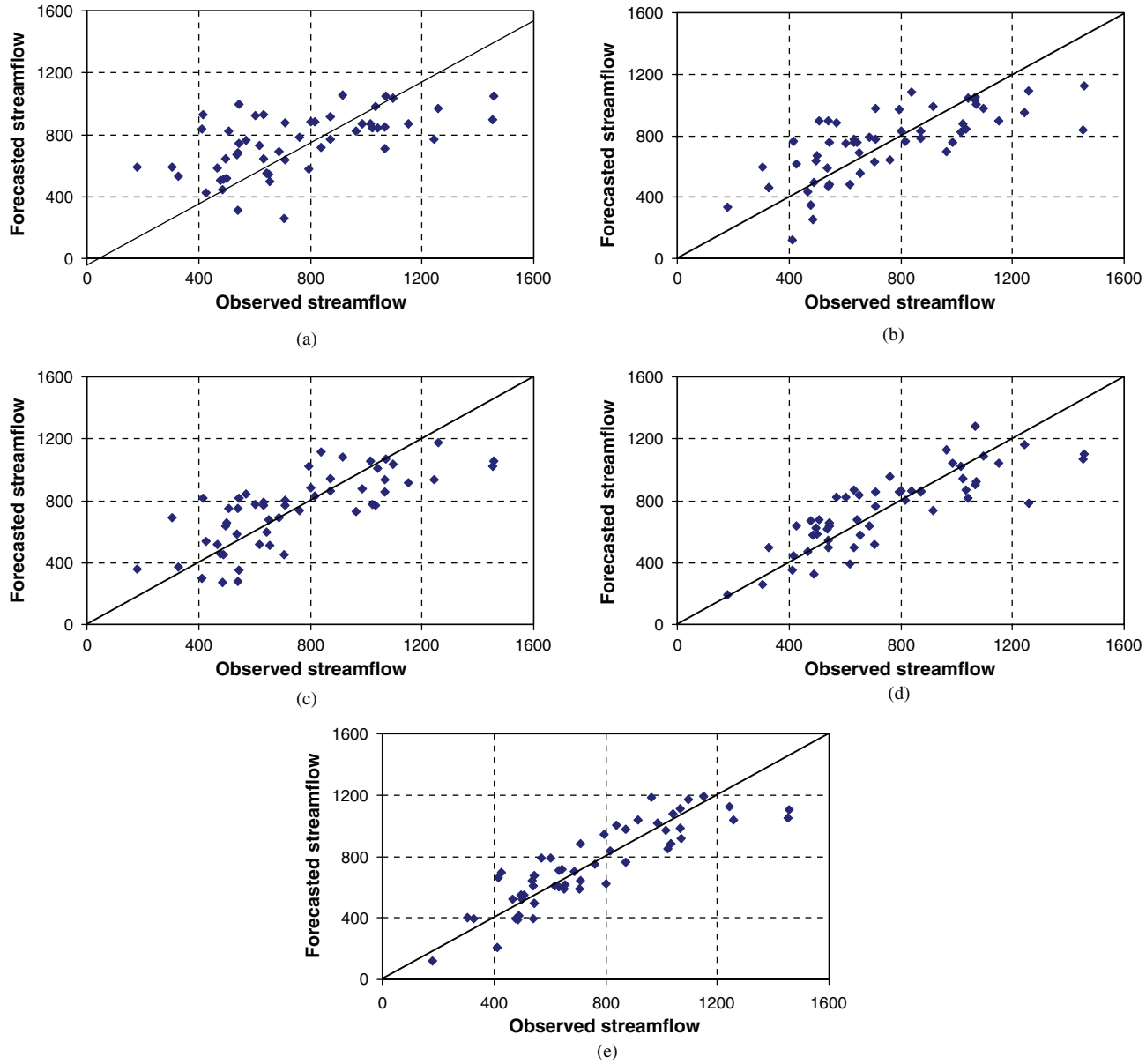

Fig. 4. Scatter plots of the drop-1 Apr.–Jul. forecasted streamflows of the Gunnison River versus the observed values for PCA models based on (a) oceanic predictors only; (b) atmospheric predictors only; (c) oceanic and atmospheric predictors; (d) hydrologic predictors only; (e) all predictors

were considered for all six rivers were determined by pooling all the potential predictors identified for the individual sites. Thus, a total of 207 potential predictors were utilized. Because this is a large number of predictors, one could trim it down by judiciously selecting a certain correlation coefficient threshold. By using a smaller number of predictors, one could directly apply the CCA method previously described. Instead, PCA was performed on all 207 predictors, and a selected number of PCs were used for CCA. To select the PCs, the variance loadings of each PC were examined (not shown). The variance dropped steadily as the number of PCs increased. The first 23 PCs accounted for approximately 90% of the variance, and each of the PCs beyond the 20th counted for less than 1% of the variances. Thus, the first 20 PCs were considered for further analysis. The first 20 PCs were entered into the CCA model one at a time (beginning with the 1st PC) until all 20 PCs were added. In each step, the sum of squared residuals (SSR) [Eq. (10)] was determined, and the PCs that caused increases in

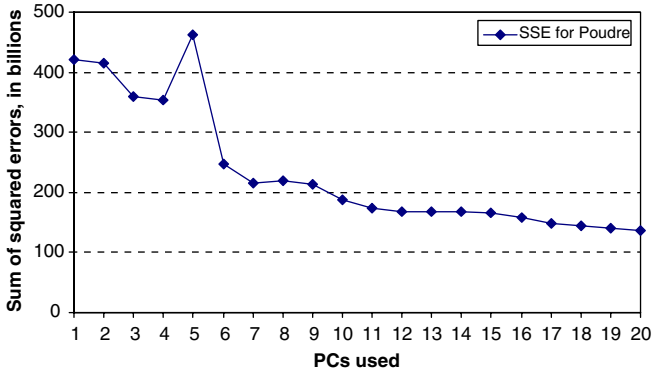

Fig. 5. SSR of Eq. (12) obtained for forecasting the Apr.–Jul. streamflows of Poudre River based on CCA models using the first 20 PCs

SSR were eliminated. For illustration, Fig. 5 shows that for the Poudre River, the SSRs obtained from CCA models fitted by adding the PCs sequentially up to 20 PCs. Adding PC5 sharply increases the SSR. For other sites, this was also observed for PC8. Consequently, these two PCs were removed from the CCA model. Meanwhile, the PCs beyond the 11th either caused additional errors or had little effect. Therefore, the CCA model used 9 PCs, namely, 1, 2, 3, 4, 6, 7, 9, 10, and 11, as the predictors. Then, the final CCA model (using 9 PCs) gave 6 eigen values: $\lambda_1 = 0.929$; $\lambda_2 = 0.781$; $\lambda_3 = 0.755$; $\lambda_4 = 0.587$; $\lambda_5 = 0.396$; and $\lambda_6 = 0.207$ (the square roots of the λ's are the canonical correlation coefficients ρ's). The significant test was then performed on the ρs. The value of the test statistic for $r = 6$ [Eq. (5)] gave 81.6, which is greater than the critical value. Therefore, the 6 canonical correlations became significant, and all the canonical variates were used in the CCA model.

The forecast performances using the CCA model were determined (not shown). Considering the various performance measures, it was clear that the better results were obtained for the Gunnison, Rio Grande, San Juan, Yampa, and Arkansas Rivers with respect to those obtained for the Poudre. In previous results (MLR and PCA for single sites), the forecasts for the Poudre and Arkansas Rivers were inferior to the other four, but in this case, only the Poudre River is inferior to the other five. The cross-correlation coefficients (not shown) indicated some underestimation relative to those obtained from the observations. The main differences occurred with cross correlations that involved the Arkansas River, although the largest underestimation was for the cross correlation between the Gunnison and Rio Grande Rivers. The scatter plot and time series (not shown) indicated a reasonable resemblance between the drop-1 streamflow forecasts and the historical flows; however, they also revealed some underestimation of the forecasted streamflows, particularly for low- and high-magnitude flows. Fig. 6 compares the drop-1 adjusted R^2s obtained for the forecasts based on the PCA, CCA, and MLR models for all sites. As expected, the R^2s for the PCA and MLR models are somewhat better (higher) than those obtained from the CCA models (except for the Arkansas River). The biggest difference in R^2 is for the San Juan River, 0.22 between PCA and CCA and 0.25 between MLR and CCA. Also, comparing the forecast skill scores obtained for PCA, CCA, and MLR suggested that PCA and MLR forecast performances are generally better than those for CCA. Comparing the cross correlations it was also clear that the correlations obtained from CCA were not better than those from PCA, and in two cases, they were much worse. This may appear to be contradicting what one may have expected, but because the forecasts obtained from PCA were generally better than those obtained from CCA, the cross correlations were also better. Also, comparing the time series of the forecasts versus the historical one as well as the corresponding scatter plots (not shown) indicated that in many cases the CCA underestimated the low flows and high flows while the PCA did a better job.

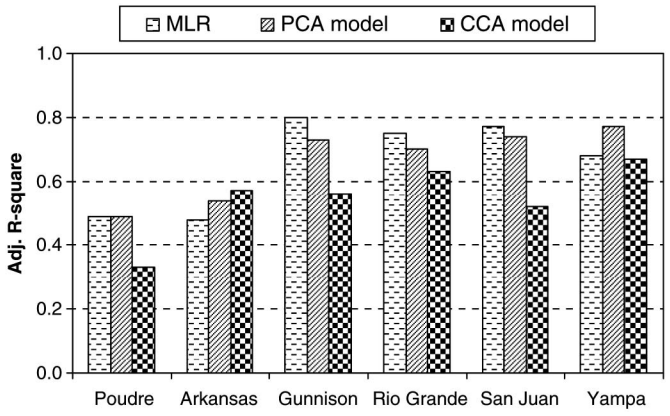

Fig. 6. Comparison of drop-1 adjusted R^2s for the MLR, PCA, and CCA models for forecasting the Apr.–Jul. streamflows for the six sites

Forecast Results for Yearly Streamflows

Forecasts for yearly October through September, January through December, February through January, and April through March streamflows have been made for the Gunnison River. We wanted to examine how PCA forecast models performed for a longer time period, i.e., a year, and for different definitions of years, because the antecedent conditions may be quite different. The procedure followed was the same as described for building and testing PCA models. Table 10 gives the parameters of the PCA models and Table 11 gives the forecast performance results. The results for the yearly periods October through September and January through December are generally comparable, while those for February through January, and April through March are markedly better. The main reason for this result is the effect that SWE plays depending on the definition of the year. For October through September, the effect of SWE of previous months (e.g., April or May) SWE is small because by the end of September, most of the snowpack accumulated since the previous fall and winter seasons has melted. For the yearly period January through December, SWE if available by December 31 (previous year) would be important for forecasting the yearly January through December streamflows, but such information is not available. On the other hand, for the yearly period February through January, SWE is available (as of February 1), and, certainly, the results show some improvement of the forecast performance. Thus, although February 1, SWE provides only partial information on the snowpack that may be available in the basin for the next year's (February through January) streamflows,

Table 10. PCA Models Obtained for Forecasting the Annual Streamflows of Gunnison River

Annual flows	Equations
Oct.–Sep.	$y = -0.670 \times \text{PC1} - 0.271 \times \text{PC5} - 0.298 \times \text{PC10} + 0.188 \times \text{PC11}$
Jan.–Dec.	$y = -0.699 \times \text{PC1} - 0.347 \times \text{PC3} + 0.143 \times \text{PC8}$
Feb.–Jan.	$y = -0.717 \times \text{PC1} - 0.350 \times \text{PC3} + 0.156 \times \text{PC8} + 0.185 \times \text{PC16}$
Apr.–Mar.	$y = -0.785 \times \text{PC1} + 0.275 \times \text{PC6} - 0.175 \times \text{PC7} + 0.165 \times \text{PC11}$

Table 11. PCA Model Performances for Forecasting Annual Streamflows of Gunnison River

		Annual streamflows			
Method	Item	Oct.–Sep.	Jan.–Dec.	Feb.–Jan.	Apr.–Mar.
Fitting	R^2	0.65	0.63	0.70	0.75
	Adjusted R^2	0.62	0.61	0.67	0.73
Drop-1	R^2	0.54	0.53	0.62	0.67
	Adjusted R^2	0.50	0.50	0.59	0.64
Fitting	Accuracy	0.55	0.57	0.60	0.62
	HSS	0.40	0.42	0.58	0.50
Drop-1	Accuracy	0.47	0.53	0.55	0.57
	HSS	0.30	0.37	0.40	0.42

it helps the forecast. Likewise, for the yearly period April through March, SWE is indeed the most important factor (predictor). Thus, it is clear that for the forecast of April through March streamflows, the forecast performances are better than for the other three yearly periods for the reasons previously explained. It is also clear that for October through September and January through December, atmospheric and oceanic factors become the most important for forecasting the flows for those yearly periods.

Final Remarks and Conclusion

The research reported herein is concerned with streamflow forecasting on a seasonal and yearly basis. Models were developed for forecasting total streamflows during April through July, and yearly streamflows for different periods. Also, different modeling schemes were adopted, and the role of hydrologic, atmospheric, and oceanic factors on forecast performance examined. We did not include in this paper results regarding forecast uncertainty. Because our procedures rely on linear regression models, estimating confidence limits on forecasts is straightforward and can be found in any standard textbook. The various forecast models, applications, and comparisons thereof led to the following conclusions:

1. Correlation analysis conducted for forecasting seasonal and annual streamflows for six rivers in Colorado indicates that hydrological variables such as SWE have the highest significant correlations, especially with seasonal April through July streamflows. SWE is still the predictor with highest correlation for forecasting yearly February through January and April through March streamflows. But for forecasting yearly October through September streamflows, SWE (April 1 or May 1) becomes less important or negligible, and for forecasting yearly January through December flows, SWE is not available. However, a number of atmospheric and oceanic variables, such as global GH, wind, RH, and SST, also have significant correlations that can be useful predictors for forecasting seasonal and yearly streamflows.
2. The forecast performances of MLR and PCA models for forecasting April through July streamflows of six major rivers in the Colorado by using hydrologic, atmospheric, and oceanic predictors are very good. The performances measures obtained from MLR and PCA models are comparable. The advantage of using MLR models over PCA is in the direct specification and identification of the various predictors in the models. In contrast, PCA models involve predictors in terms of principal components. On the other hand, the advantage of using PCA models has been in a better reproduction of historical cross correlations among sites (compared with MLR models).
3. It has shown that atmospheric and oceanic factors play a significant role in forecasting seasonal and yearly streamflows in Colorado rivers. For example, for forecasting the April through July streamflows for the Gunnison River using only atmospheric and oceanic predictors, the drop-1 adjusted R^2 is approximately 0.5, which is pretty good. Likewise, forecasting the yearly October through September and January through December streamflows is essentially based on atmospheric and oceanic predictors, yet the results are quite good (the drop-1 adjusted R^2 is also 0.5 in both cases). It is concluded that atmospheric and oceanic predictors alone can predict reasonably well the streamflow variations of the Gunnison River on seasonal and yearly timescales.
4. PCA models were applied for forecasting yearly October through September, January through December, February through January, and April through March streamflows. It has been shown that good forecasting performance can be achieved for yearly timescales. Better results are obtained for forecasting the yearly February through January, and April through March than for the other two because the former has the advantage of including hydrologic predictors, such as SWE, whereas for October through September, such information is less significant or not useful because for the year that begins in October, most if not all potential snowpack in the basin may have already melted. Thus, the forecasts for the yearly October through September rely almost solely on atmospheric and oceanic data. Likewise, the forecast for the yearly streamflows during January through December relies largely on atmospheric and oceanic predictors because SWE is not available in December of the previous year, which could help in obtaining better forecast.
5. We applied CCA to forecasts for the April through July streamflows at the six study sites jointly. The forecast performance obtained based on CCA is good. However, the results are inferior to those obtained from PCA applied individually at each site. This is also the case when comparing cross correlations. Thus, it is concluded that in forecasting the April through July streamflows for Colorado rivers using CCA we did not find any advantage over the forecasts obtained using PCA at single sites.
6. In applying the various forecasting methods for six rivers in Colorado, namely, Poudre, Arkansas, Rio Grande, San Juan, Gunnison, and Yampa, it has been clear that much better forecast performance is achieved for the last four rivers than for the Poudre and Arkansas Rivers. It appears that the main reason for this notable difference in forecast performance is because for the Poudre and Arkansas Rivers the (average) correlations between the flows and hydrologic predictors (SWE and PDSI) is 0.48, while for the other four rivers it is 0.68.

Acknowledgments

The authors would like to acknowledge the financial support of the project Predictability of the Upper Colorado River Streamflows funded by the Colorado Water Resources Research Institute and the U.S. Geological Survey. In addition, thank you to the reviewers and the associate editor for making important suggestions to improve the paper.

References

Canon, J., Gonzalez, J., and Valdes, J. (2007). "Precipitation in the Colorado River Basin and its low frequency associations with PDO and ENSO signals." *J. Hydrol.*, 333(2-4), 252–264.

Cayan, D. R., Dettinger, M. D., Diaz, H. F., and Graham, N. (1998). "Decadal variability of precipitation over western North America." *J. Clim.*, 11, 3148–3166.

Cayan, D. R., and Webb, R. H. (1992). "El Niño/southern oscillation and streamflow in the western United States." *Historical and paleoclimate aspects of the Southern Oscillation*, H. F. Diaz and V. Markgraf, eds., Cambridge University Press, Cambridge, UK, 29–68.

Clark, M. P., Serreze, M. C., and McCabe, G. J. (2001). "Historical effects of El Niño and La Niña events on seasonal evolution of the montane snowpack in the Columbia and Colorado River Basins." *Water Resour. Res.*, 37(3), 741–757.

Dettinger, M. D., Cayan, D. R., Diaz, H. F., and Meko, D. (1998). "North-south precipitation patterns in western North America on interannual-to-decadal time scales." *J. Clim.*, 11, 3095–3111.

Donald, B. A., and Lindgren, W. (1996). *Statistics: Theory and methods*, 2nd Ed., Duxbury, Pacific Grove, CA, 635.

Eldaw, A. K., Salas, J. D., and Garcia, L. A. (2003). "Long range forecasting of the Nile River flow using large scale oceanic atmospheric forcing." *J. Appl. Meteorol.*, 42(7), 890–904.

Eltahir, E. A. B. (1996). "El Niño and the natural variability in the flow of the Nile River." *Water Resour. Res.*, 32(1), 131–137.

Grantz, K., Rajagopalan, B., Clark, M., and Zagona, E. (2005). "A technique for incorporating large-scale climate information in basin-scale ensemble streamflow forecasts." *Water Resour. Res.*, 41, W10410.

Haltiner, J. P., and Salas, J. D. (1988). "Short-term forecasting of snowmelt runoff using ARMAX model." *Water Resour. Bull.*, 24(5), 1083–1089.

Hamlet, A. F., and Lettenmaier, D. P. (1999). "Effects of climate change on hydrology and water resources in the Columbia River Basin." *J. Am. Water Resour. Assoc.*, 35(6), 1597–1623.

Hidalgo, H. G., and Dracup, J. A. (2003). "ENSO and PDO effects on hydroclimate variations of the Upper Colorado River Basin." *J. Hydrometeorol.*, 4, 5–23.

Higgins, R. W., Leetmaa, A., Xue, Y., and Barnston, A. (2000). "Dominant factors influencing the seasonal predictability of United States precipitation and surface temperature." *J. Clim.*, 13, 3994–4017.

Kalnay, E., et al. (1996). "The NCEP/NCAR 40-year reanalysis project." *Bull. Am. Meteorol. Soc.*, 77(3), 437–471.

Manly, B. F. J. (1994). *Multivariate statistical methods—A primer*, 2nd Ed., Kluwer, Norwell, MA.

Mantua, N. J., Hare, S. R., Zhang, Y., Wallace, J. M., and Francis, R. C. (1997). "A Pacific decadal climate oscillation with impacts on salmon." *Bull. Am. Meteorol. Soc.*, 78, 1069–1079.

Maurer, E. P., and Lettenmaier, D. P. (2003). "Predictability of seasonal runoff in the Mississippi River Basin." *J. Geophys. Res.*, 108.

Maurer, E. P., Lettenmaier, D. P., and Mantua, N. J. (2004). "Variability and potential sources of predictability of North American runoff." *Water Resour. Res.*, 40, W09306.

McCabe, G. J., and Dettinger, M. D. (1999). "Decadal variations in the strength of ENSO teleconnections with precipitation in the western United States." *Int. J. Climatol.*, 19, 1399–1410.

McCabe, G. J., and Dettinger, M. D. (2002). "Primary modes and predictability of year-to-year snowpack variations in the western United States from teleconnections with Pacific Ocean climate." *J. Hydrometeorol.*, 3, 13–25.

McCabe, G. J., Palecki, M. A., and Betancourt, J. L. (2004). "Pacific and Atlantic Ocean influences on multidecadal drought frequency in the United States." *Proc., National Academy of Sciences*, Washington, DC, 4136–4141.

Moss, M. E., Pearson, C. P., and McKerchar, A. I. (1994). "The Southern Oscillation index as a predictor of the probability of low streamflows in New Zealand." *Water Resour. Res.*, 30, 2717–2713.

Piechota, T. C., and Dracup, J. A. (1996). "Drought and regional hydrologic variation in the United States: Associations with the El Niño-Southern Oscillation." *Water Resour. Res.*, 32(5), 1359–1373.

Piechota, T. C., Dracup, J. A., and Fovell, R. G. (1997). "Western United States streamflow and atmospheric circulation patterns during El Niño-Southern Oscillation." *J. Hydrol.*, 201(1-4), 249–271.

Regonda, S. K., Rajagopalan, B., Clark, M., and Zagona, E. (2006). "A multimodel ensemble forecast framework: Application to spring seasonal flows in the Gunnison River Basin." *Water Resour. Res.*, 42, W09404.

Ropelewski, C. F., and Halpert, M. S. (1987). "Global and regional scale precipitation patterns associated with El Niño/Southern Oscillation." *Mon. Weather Rev.*, 115, 1606–1626.

Salas, J. D., et al. (2005). "Characterizing the severity and risk of drought in the Poudre River, Colorado." *J. Water Resour. Plng. and Mgmt.*, 131(5), 383–393.

Slack, J. R., and Landwehr, J. M. (1992). "Hydro-Climatic Data Network: A. USGS streamflow data set for the United States for the study of climatic variations from 1974 to 1988." *Rep. 92-129*, USGS Open File, 193.

Sveinsson, O. G. B., Lall, U., Gaudel, J., Kushnir, Y., Zebiak, S., and Fortin, V. (2008). "Analysis of climatic states and atmospheric circulation patterns that influence Quebec spring streamflows." *J. Hydrol. Eng.*, 13(6), 411–424.

Tootle, G. A., and Piechota, T. C. (2006). "Relationships between Pacific and Atlantic ocean sea surface temperatures and United States streamflow variability." *Water Resour. Res.*, 42.

Tootle, G. A., Piechota, T. C., and Singh, A. K. (2005). "Coupled oceanic-atmospheric variability and United States streamflow." *Water Resour. Res.*, 41.

Tootle, G. A., Singh, A. K., Piechota, T. C., and Farnham, I. (2007). "Long lead-time forecasting of United States streamflows using partial least squares regression." *J. Hydrol. Eng.*, 12(5), 442–451.

Wang, D. C., and Salas, J. D. (1991). "Forecasting streamflow for Colorado river systems." *Completion Rep. No. 164*, Colorado Water Resources Research Institute, Denver.

Wilks, D. S. (2006). *Statistical methods in the atmospheric sciences*, 2nd Ed., Elsevier, Atlanta, 519–522.